One-step synthesis of poly(ethylene oxide)/gold nanocomposite hydrogels and suspensions using gamma-irradiation

Ivan Marić[1], Nataša Šijaković Vujičić[2], Anđela Pustak[1], Marijan Gotić[3], Tanja Jurkin[1]*

[1]*Radiation Chemistry and Dosimetry Laboratory, Division of Materials Chemistry, Ruđer Bošković Institute, Bijenička 54, 10 000 Zagreb, Croatia*

[2]*Laboratory for Supramolecular Chemistry, Division of Organic Chemistry and Biochemistry, Ruđer Bošković Institute, Bijenička 54, 10 000 Zagreb, Croatia*

[3]*Laboratory for Molecular Physics and Synthesis of New Materials, Division of Materials Physics, Ruđer Bošković Institute, Bijenička 54, 10 000 Zagreb, Croatia*

Abstract

Poly(ethylene oxide) (PEO)/gold nanocomposite hydrogels and suspensions were synthesized by γ-irradiation of PEO and Au^{3+} aqueous solutions to a dose of 50 kGy under inert atmosphere and without addition of 2-propanol, depending on the initial concentration of Au^{3+} and pH of solutions. The pH of the initial solutions had the major influence on the formation of PEO/Au nanocomposite hydrogels vs. suspensions. The pH and Au^{3+} initial concentration determined the AuNPs size and suspension stability, as determined by UV-Vis spectroscopy. The neutral pH favored the formation of stable suspensions with the smallest gold nanoparticles (AuNPs), whereas unstable suspensions and bigger nanoparticles (NPs) were obtained at acidic pH and by increasing Au^{3+} initial concentration. On irradiation at alkaline conditions PEO/AuNPs hydrogels were produced in one-pot synthesis method - by simultaneous crosslinking of PEO chains and reduction/synthesis of Au nanoparticles. Scanning electron microscopy of nanocomposite gels revealed the gold nanoparticles embedded in PEO matrix with homogenous distribution. The thermal and viscoelastic properties of PEO/AuNPs gels depended on the initial Au^{3+} concentration, that is on amount of AuNPs synthesized inside gels. Lower particle content resulted in gels with generally higher melting and crystallization temperatures as well as higher storage moduli, yield points and flow points than pure PEO gel. The optimal amount were up to 1 wt% Au for obtaining

stronger gels, whereas higher amount of NPs, because of NPs agglomeration, lead to deterioration of gel properties and significant weakening of gel.

Keywords: gold nanoparticles, PEO/gold nanocomposite hydrogels, gamma-irradiation, one step synthesis, rheological properties, thermal properties

*Corresponding author: Tanja Jurkin, Ruđer Bošković Institute, Bijenička 54, 10000 Zagreb, Croatia, phone: +385 1 4571 255, *e-mail address*: tjurkin@irb.hr

# I. Marić and N. Šijaković Vujičić are equally contributing main authors

1. Introduction

Gold nanoparticles (AuNPs) possess unique electrical and optical properties, depending on their size and shape. AuNPs have found applications in analytical chemistry (Kwon et al., 2012), catalysis (Ide et al., 2014; Zope et al., 2010) and in biomedicine (Dykman and Khlebtsov, 2012; Jiao et al., 2011; Tiwari et al., 2011). They are used as contrast agents (Hainfeld et al., 2006; Reuveni et al., 2011), biosensors (Rojanathanes et al., 2008; Zhu et al., 2019), for photothermal therapy, drug and gene delivery (Jahangirian et al. 2019; Llevot and Astruc, 2012) immunoassays, tissue engineering (Hasan et al., 2018; Navaei et al., 2016; Nirwan et al., 2019; Shevach et al., 2014) and as radiosensitisation agents (Butterworth et al., 2012; Hainfeld et al., 2004; Hanžić et al, 2018; Jain et al., 2011; Rosa et al., 2017).

γ-irradiation is proven to be a powerful tool for synthesis of various nanoparticles (Gotić et al. 2009; Jurkin et al. 2016a; Mikac et al. 2019; Marić et al., 2019) of controlled size and shape, including gold NPs. The main principle of AuNPs synthesis by γ-irradiation of auric (Au^{3+}) salt aqueous solutions is reduction of gold cations by hydrated electrons, e^-_{aq}, ($E^o(H_2O/e^-_{aq})$ = -2.87 V_{NHE}) and proton radicals, $H^\bullet$, ($E^o(H^+/H^\bullet)$ = -2.30 V_{NHE}) which are strong reducing agents formed on water radiolysis (Abidi and Remita, 2010; Gachard et al., 1998; Dey et al., 2011). Because of high energy and penetration of γ-radiation strong reducing species are formed homogenous through the solution, resulting in homogenous reduction and AuNPs nuclei formation, hence smaller NPs size, what is very difficult to achieve by

admixing external conventional chemical reducing agents. Because the oxidizing species, such as hydroxyl radical ($HO^{\bullet}$) ($E^{o}(^{\bullet}OH/H_2O)$ = +2.34 V_{NHE}) are also formed on water radiolysis, to ensure the strong reducing conditions irradiation is performed in deoxygenated solutions and with addition of scavengers of hydroxyl radicals, like 2-propanol. The formed 2-propanol radicals can also reduce gold cations ($E^{o}((CH_3)_2CO/(CH_3)_2C^{\bullet}OH$ = -1.8 V_{NHE} at pH=7). In addition, the presence of small organic molecules, surfactants or polymers (Al Gharib et al., 2019; Belloni et al., 1998; Hoppe et al., 2006) stabilizes and restricts NPs growth and prevents aggregation through steric or electrostatic repulsion. They can also act as additional reducing agents. The size and shape of formed AuNPs can be controlled by the irradiation dose, dose rate, as well as polymer/surfactant concentration (Hanžić et al., 2015; Jurkin et al., 2016b; Li et al., 2007; Misra et al., 2012).

γ-irradiation is also suitable for synthesis of NPs within the three-dimensional polymer network, thus restricting the growth of NPs inside network cavities, and producing nanocomposite hydrogels of specific properties. As a rule, the composite gels are synthesized using two steps methods. γ-irradiation can induce crosslinking of polymer in the presence of previously prepared NPs or γ-irradiation is used to synthesize NPs within previously prepared polymer gel (Jurkin et al. 2013; Jovanović et al., 2011; Krklješ et al., 2007; Spasojević et al. 2015). On the other hand, there is a particular interest for the one-step γ-irradiation synthesis of nanocomposite gels. One-step synthesis takes an advantage of simultaneous crosslinking of polymer chains with the formation of network and reduction of metal salts and formation of NPs. This is quicker, simpler, and results in small NPs size and narrow size distribution, as well as homogenous distribution of NPs through the polymer matrix. The advantages of γ-irradiation synthesis of gels is clean and homogenous reaction initiation as well as sterility of the final product. AuNPs can enhance the optical, mechanical, electrical, thermal and biological properties of gel. AuNPs nanocomposite hydrogels have found application in drug delivery and tissue engineering. They have been used for bone and cardiac tissue regeneration, because they promote osteogenic differentiation, increase cell proliferation rates and due to special electrical properties help in synapse formation (Hasan et al., 2018; Navaei et al., 2016; Ravichandran et al., 2014; Shevach et al., 2014; Thoniyot et al., 2015).

In our previous paper we successfully synthesized AuNPs using γ-irradiation in the presence of citrates (Hanžić et al., 2015) and within the microemulsion droplets to control AuNPs size and dispersion (Jurkin et al., 2016b). We have shown that in both cases the

AuNPs could be formed at highly oxidizing conditions, *i.e.* in the presence of oxygen and without using scavengers such as 2-propanol. In the current work we studied the impact of poly(ethylene oxide) (PEO) on the γ-irradiation synthesis PEO/AuNPs nanocomposite hydrogels and AuNPs suspensions. PEO is a semicrystalline, hydrophilic and biocompatible polymer with numerous applications in pharmaceuticals and biomedicine, for instance, as wound dressing and hydrogel for active substance release. Because of its hydrophilicity and biocompatibility it is used for surface modification of NPs to prolong blood circulation time, reduce non-specific interactions and for NPs functionalization (Tiwari et al., 2011). Like other polymers it is also used for stabilization and controlling NPs size during synthesis. Upon γ-irradiation of its aqueous solutions, PEO easily crosslinks and forms macroscopic "wall-to-wall" hydrogels (Jurkin and Pucić, 2012, 2013; Savaş and Güven, 2002; Ulański et al., 1995a, 1995b).

Thus, in this work we explored the ability of γ-irradiation technique for one-step synthesis of PEO/AuNPs nanocomposite hydrogels. We optimized experimental conditions, regarding the pH and initial Au^{3+} salt concentration, and at alkali conditions the γ-irradiation of PEO/Au^{3+} aq. solutions resulted in one-step formation of PEO/AuNPs nanocomposite gels. The influence of Au^{3+} concentration on thermal and rheological properties of such synthesized PEO/AuNPs nanocomposite gels was studied. The effect of pH and initial Au^{3+} salt concentration on the AuNPs size and stability of suspensions obtained on irradiation at neutral and acidic conditions were also investigated.

2. Materials and methods

2.1 Chemicals

All chemicals were of analytical purity and used as received. Gold(III) chloride trihydrate ($HAuCl_4 \cdot 3H_2O$), ≥ 99.9% trace metals basis was supplied by *Sigma Aldrich*. Sodium hydroxide (p.a.) by *LachNer*, 2-propanol (CROMASOLV, for HPLC, ≥99.9%) by *Sigma-Aldrich*/*Honeywell*, PEO of viscosity average molecular weight (M_v) 400,000 by *Sigma-Aldrich* and Milli-Q deionized water with a resistivity 18 MΩ cm at 25°C was used. $HAuCl_4$ 4 wt% stock solution was prepared by dissolving 1 g of $HAuCl_4 \cdot 3H_2O$ in 25 mL Mili-Q water.

2.2 Synthesis of samples

Gold(III) chloride trihydrate salt was used as a precursor for the synthesis of gold nanoparticles. Firstly, 1.85 wt% PEO aqueous stock solution was prepared. Then 4 wt% $HAuCl_4$ aqueous solution was added to 1.85 wt% PEO solution in an amount to obtain solutions with 0.5, 1, 2, 5 and 10 wt% of Au^{3+} ions in relation total PEO and Au mass. This corresponds to initial Au^{3+} with concentrations of $4.69 \cdot 10^{-4}$, $9.32 \cdot 10^{-4}$, $1.85 \cdot 10^{-3}$, $4.50 \cdot 10^{-3}$ and $8.61 \cdot 10^{-3}$ mol dm^{-3}, respectively (Figure 1, Table 1). The pH of solutions was adjusted to different values ranging from 3 to 11 with slowly adding 2 M NaOH aqueous solution during vigorous stirring. pH was measured with Mettler Toledo SevenCompact S220 pH meter previously calibrated with buffers having pH of 4.01, 7.00, 9.21 and 11.00. No scavenger, like 2-propanol, was added to the solutions. Such prepared solutions were bubbled with nitrogen through rubber septa for 30 min in order to remove dissolved oxygen before γ-irradiation. γ-irradiation of deoxygenated suspensions in a septum-closed glass flasks was performed at room temperature in a ^{60}Co γ-irradiation facility located in the Radiation Chemistry and Dosimetry Laboratory at the Ruđer Bošković Institute. Suspensions were irradiated to the absorbed dose of 50 kGy at a dose rate of ~27 kGy h^{-1}. The detailed experimental conditions and products obtained on irradiation are given in Table 1.

2.3 Characterization of samples

Synthesized samples were characterized as synthesized gels (rheological measurements), as dried gels (DSC, SEM) and suspensions (SEM, UV-Vis). Obtained gels were dried under vacuum at room temperature.

Size and morphology of the samples were investigated using a field emission scanning electron microscope (FE SEM), model JSM-7000F, manufactured by *JEOL Ltd.* and connected to the EDS/INCA 350 (energy dispersive X-ray analyzer) manufactured by *Oxford Instruments*.

The UV-Vis spectra of gold suspensions were recorded using a UV/VIS/NIR spectrometer *Shimadzu* model UV-3600. The quartz cells having 1cm optical path length were used. The gold particle size was calculated from UV-Vis spectra using the procedure presented by Haiss et al. (2007) and by Khlebtsov (2008).

Differential scanning calorimetry (DSC) thermograms were recorded using *PerkinElmer Diamond* calorimeter, calibrated with In and Zn standards and operating in a

dynamic mode. Samples of dried gel (5-10 mg) were sealed into Al pans. Two heating and cooling cycles at temperatures ranging from -40 °C to 100 °C in an extra pure nitrogen environment were performed for each sample at a rate of 10 °C min^{-1}. The first heating cycle was performed in a range 22 °C to 100 °C. For each synthesized gel three specimens were recorded. The temperatures and enthalpies of melting and crystallization were determined from both first and the second heating and first cooling cycles, and their averages are presented. The degree of crystallinity ($w_{c,H}$) of PEO gels and PEO/Au nanocomposite gels was calculated using Eq. 1.

$$w_{c,H} = \Delta H_m / \Delta H_{m,0} \quad (1)$$

where ΔH_m is the enthalpy of melting per gram of sample recalculated on pure PEO mass and $\Delta H_{m,0}$ is the enthalpy of melting per gram of the 100% crystalline PEO (theoretical value). For $\Delta H_{m,0}$ the value of 197.0 J g^{-1} was used (Wunderlich 1973, Menczel and Prime, 2009).

The mechanical properties of gels are described using oscillatory rheology. The storage (G') and loss (G'') moduli of the nanocomposite gels were determined with a mechanical spectrometer (Anton Paar MCR 302, Stuttgart, Germany), using a steel plate−plate geometry (PP25, Anton Paar, Graz-Austria) equipped with a true-gap system and the data were collected using RheoCompass software. The sample temperature was controlled through a Peltier temperature control located on the base of the geometry and with a Peltier-controlled hood (H-PTD 200). A piece of a gel sample (1 mm thick slice) was placed on the base plate of the rheometer, and the plate was set using the true-gap function of the software. Thus, after 5 min at 25 °C, the G' and G'' moduli were measured always within the linear viscoelastic region (LVR). After 5 min at 25 °C, the yield stress of the gels was determined by applying a strain (γ) sweep between 0.01 % and 100 %. Rheological properties of a gel material are independent of strain up to yield strain, and beyond yield strain the rheological behavior is nonlinear. Three interval thixotropy test is a standard test which allows tracking of material response resulting from stepwise changes in shear strain making it the most appropriate method for structure recovery tests. In the thixotropic experiments, rheological measurements were conducted on gels at 25 °C under initial conditions at which they were in their linear viscoelastic regimes (a strain of 0.5 % and angular frequency of 5 rad/s) for 680 s to establish baseline values for G' and G''. In studies with gels viscoelastic recovery was observed after the cessation of destructive strain. Frequency sweeps (0.05–100 rad/s) were

subsequently performed at 25 °C at a strain value within LVR to investigate the time-dependent deformation behavior of gels.

3. Results and discussion

By γ-irradiation of PEO and Au^{3+} aqueous solutions under inert atmosphere to a dose of 50 kGy, Au^{3+} ions were successfully reduced without addition of 2-propanol. Depending on the pH γ–irradiation of yellow PEO/Au^{3+} precursor solutions resulted in formation of red to purple PEO/Au suspensions or red to purple nanocomposite hydrogels (Figure 1, Table 1). pH below 8 favoured formation of AuNPs suspensions, while permanent shaped nanocomposite hydrogels were obtained at more alkaline conditions (pH = 10-11). At pH range 8-10.5 the formation of suspensions *vs.* gels also depended on the initial concentration of gold(III) salt. At pH = 8-9 only solutions containing 1 % Au^{3+} resulted in formation of hydrogels.

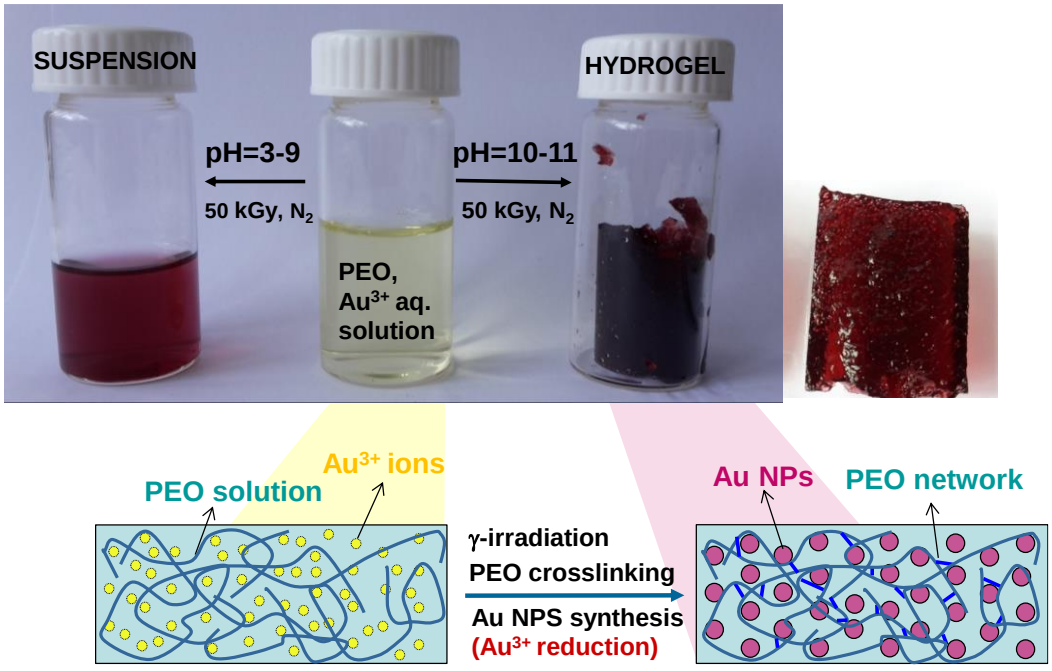

Figure 1. Photographs of synthesis procedure for preparation of PEO/AuNPs suspensions or PEO/AuNPs nanocomposite hydrogels by -irradiation, with schematic representation of one step synthesis method for preparation of PEO/Au nanocomposite hydrogels.

Table 1. The detailed experimental conditions, products obtained (suspensions or gels) and the size of synthesized AuNPs as determined from UV-Vis spectra and SEM images.

Initial wt% Au^{3+} (in relation to total PEO and Au mass)	pH before irradiation	pH after irradiation	AuNPs size from UV-Vis spectra* / nm (according to Haiss et al. 2007)	AuNPs size from Vis spectra** / nm (according to Khlebtsov, 2008)	AuNPs size from SEM images*** D_{mean} / nm and standard deviation (s / nm)	Colour and stability of suspension/gel
0	3.83	-	-	-	-	gel
0	8-9	-	-	-	-	gel
0	10.5-11.0	-	-	-	-	gel
0.5	10.8-11.1	-	-	-	-	purple gel
1	3.76	2.83	51.8	47.9	28.7 (8.7)	red suspension, unstable
1	4.6	2.8	49.4	45.7	34.8 (8.4)	red suspension, unstable with time
1	5.15	3.22	9.1	24.2	18.3 (3.9)	red (slightly purple) suspension, unstable with time
1	6.78	3.39	8.0	20.6	13.7 (1.9)	red suspension, stable
1	8.6-8.9	-	-	-	-	red gel
1	10.8-11.0	-	-	-	24.3 (4.3)	purple gel
2	3.24	2.50	106.4 + 140.2	112.4 + 173.4	24.0 (8.1) + 124.1 (9.9)	pink-light brownish suspension, unstable
2	6.84	3.41	8.8	27.4	19.1 (4.4)	red-purple suspension, unstable with time
2	8.54	3.18	44.3	41.1	22.7 (4.8)	purple suspension, unstable
2	10.6-11.0	-	-	-	-	dark purple gel
5	6.77	2.93	60.3	56.0	37.7 (9.8)	purple suspension, unstable
5	8.69	2.82	-	-	-	dark grey suspension, unstable
5	10.5–11.0	-	-	-	-	dark purple gel
10	10.67-10.9	-	-	-	35.4 (16.2) + aggregated 100-300	dark purple gel

*UV-Vis determination of gold nanoparticle size using the procedure presented by Haiss et al. (2007). The method is based on the relative A_{SPR}/A_{450} ratio.

**UV-Vis determination of AuNPs size using the procedure presented by Khlebtsov (2008).

***Particle diameters were measured using ImageJ software from SEM images and particle size distributions were calculated. *s* is a standard deviation.

3.1 Size and morphology characterization of PEO/AuNPs gels and suspensions

Suspensions obtained by irradiation at pH < 8 were of different color and stability depending on the pH of the precursor solution. They were brownish-pink to red and purple in color by irradiation at acidic, neutral and slightly alkali range, respectively. The UV-Vis spectra of obtained suspensions and photographs showing the color of the suspensions are given in Figure 2. The pH and Au^{3+} concentration, and hence PEO/Au^{3+} ratio, markedly influenced AuNPs size and suspension stability. The position of surface plasmon resonance (SPR) band for sample synthesized at neutral solutions and with 1 wt% Au^{3+} was around 522 nm. By moving the pH to more alkali or acidic range, and by adding more gold ions the position of SPR band shifted to higher values. Generally, the position, width and intensity of SPR band depend on the AuNPs particle size, shape, concentration, surface charge, refractive index of the surrounding medium and interparticle interactions. The position of SPR bands has been regularly used for the determination of particle size. For spherical particles the position of SPR band decrease with the particles size (Heiss et al., 2007). In this work we calculated particle size using the procedure presented by Heiss et al. (2007) which is based on the relative A_{SPR}/A_{450} ratio, and method presented by Khlebtsov (2008). The results are given in Table 1. Neutral pH favored the formation of stable red AuNPs suspensions of very small NPs. The AuNPs synthesized at pH ~7 and with initial 1 wt% of Au^{3+} (initial concentration $9.32 \cdot 10^{-4}$ mol dm^{-3}) showed the smallest particle size (8.0 nm), as the red color of the colloid solution suggested. This was the most stable suspension, stable even after few months. The AuNPs synthesized at highly acidic conditions were around five times larger and very unstable. In addition, AuNPs size increased several times with increase of Au^{3+} concentration from $9.3 \cdot 10^{-4}$ mol dm^{-3} (1 wt% Au^{3+}) to $4.5 \cdot 10^{-3}$ mol dm^{-3} (5 wt% Au^{3+}). Suspension obtained by irradiation of initial 2 wt% Au^{3+} at pH = 3.24 obviously contains AuNPs of wide range of distributions, as evidenced by complex UV-Vis spectrum (convolution of several spectra).

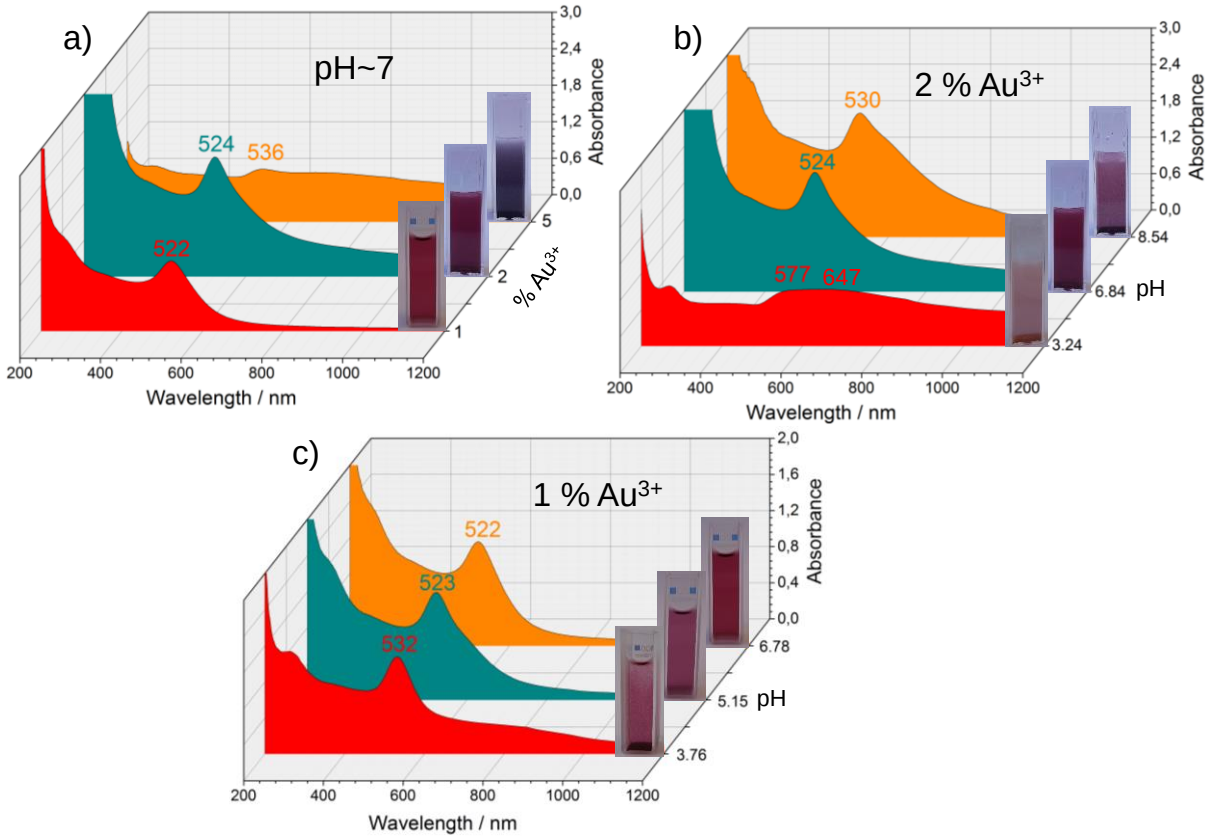

Figure 2. UV-Vis spectra od suspensions obtained by γ-irradiation of PEO aq. solution containing: a) different amount of Au^{3+} at ~ pH = 7, b) 2 wt% of initial Au^{3+} at various pH, and c) 1 wt% of initial Au^{3+} at various pH. The pH of solutions was adjusted with 2 M NaOH aqueous solution. All spectra are of 3x diluted suspensions, except of one with 5% Au^{3+} which is 6x diluted. Inset photos show the color and stability of AuNPS suspensions (3x diluted).

Figure 3. shows the SEM images and the corresponding particle size distribution of suspensions obtained by 50 kGy irradiation of PEO solution with various amount of Au^{3+} at different pH. The smallest spherical particles (13.7 nm) were obtained at 1 wt% Au^{3+} at neutral pH (Fig. 3d). The particles obtained at acidic conditions (1%, pH=3.76) and from more concentrated Au^{3+} solutions (5%, pH~7) were bigger, with sizes 28.7 nm, and 37.7 nm, respectively. The trend in increase of AuNPs size with decreasing pH and increase of precursor concentration is similar to those already observed from the UV-Vis spectra. Suspension obtained by irradiation of initial 2 wt% Au^{3+} at pH = 3.24 contains small spherical ~24 nm (Fig. 3e), but also big spherical particles around 124 nm in size (Fig. 3f), as well as some big plate like particles (hexagon tiles 342 nm and triangular tiles ~267 nm), as

evidenced also by complex UV-Vis spectra. Few bigger spherical or plate like/hexagonal particles, with diameters of 100 nm and more, are visible in all suspensions with 2 wt% and 5 wt% Au^{3+}.

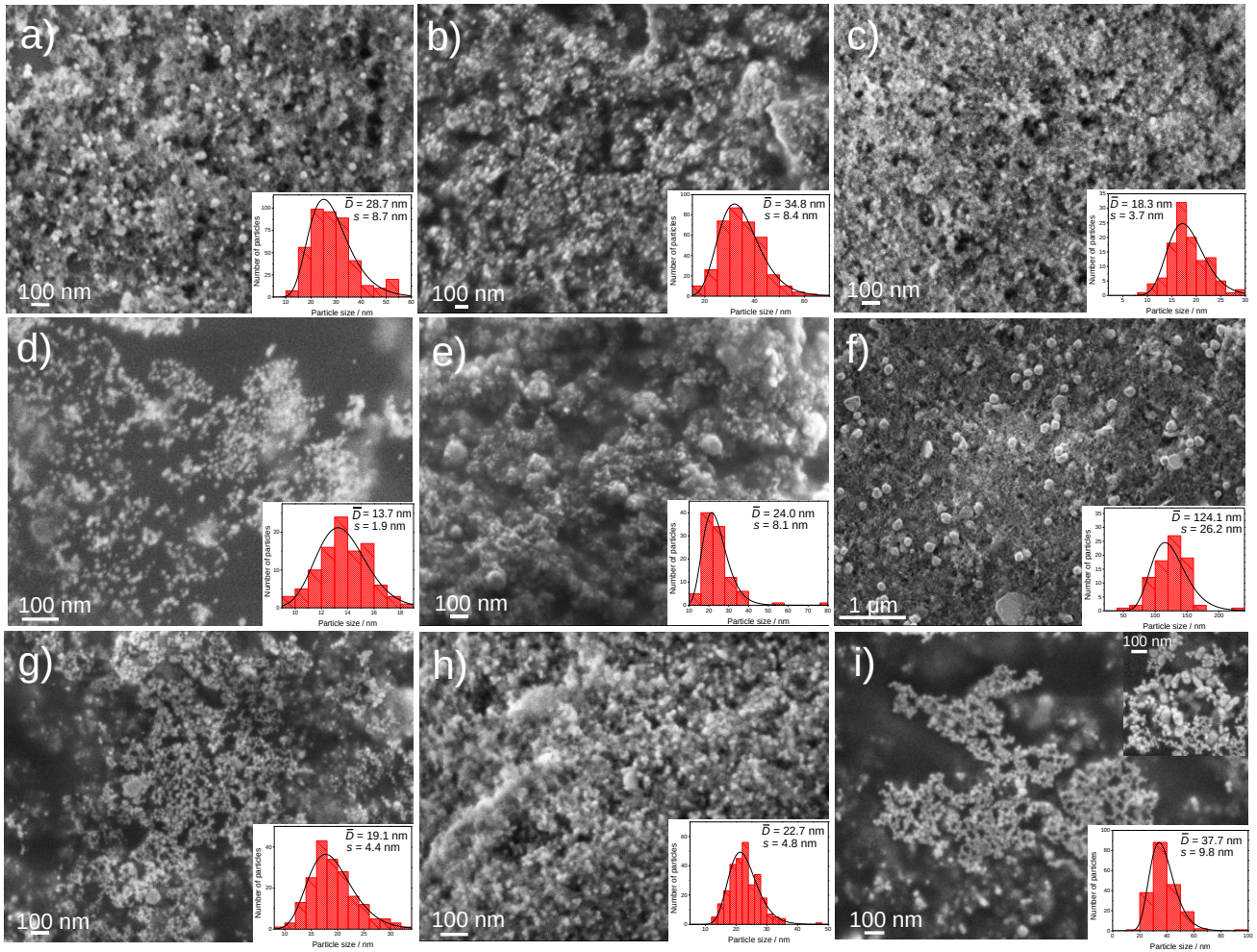

Figure 3. SEM images and corresponding particle size distributions of Au suspensions obtained by irradiation of PEO solutions with: 1 wt% Au^{3+} at pH=3.76 (a), 1 wt% Au^{3+} at pH=4.6 (b), 1 wt% Au^{3+} at pH=5.15 (c), 1 wt% Au^{3+} at pH=6.78 (d), 2 wt% Au^{3+} at pH=3.24 (e and f), 2 wt% Au^{3+} at pH=6.84 (g), 2 wt% Au^{3+} at pH=8.54 (h), 5 wt% Au^{3+} at pH=6.77 (i).

As already said the basic mechanism of AuNPs formation by irradiation of aq. solution proceeds via reduction of Au^{3+} ($Au^{III}Cl_4^-$) with hydrated electrons, e_{aq}^-, (also in a smaller amount with proton radical, $H^\bullet$) formed on water radiolysis (Abidi and Remita, 2010; Gachard et al., 1998; Dey et al., 2011.)

$$H_2O \rightsquigarrow e_{aq}^-, H^\bullet, {}^\bullet OH, H_2O_2, HO_2^\bullet, H_2, O_2^{\bullet -}, H_3O^+ \quad (2)$$

This process of reduction of $Au^{III}Cl_4^-$ to $Au^{II}Cl_4^{2-}$, $Au^{I}Cl_2^-$, and finally to Au^0 is pretty complex, it occures in several steps, but it can be presented via this simplified process:

$$Au^{3+} + e_{aq}^- \rightarrow Au^{2+} \rightarrow Au^+ \rightarrow Au^0 \text{ atoms} \rightarrow \text{oligomers} \rightarrow Au_n^{X+} \text{clusters} \rightarrow Au_n \text{ NPs} \quad (3)$$

To ensure the reducing conditions in these experiments irradiation was performed in deoxygenated solutions, to prevent the conversion of highly reactive reducing radicals, i.e. hydrated electrons, e_{aq}^-, and $H^\bullet$ with dissolved oxygen to corresponding $O_2^{\bullet -}$ and $HO_2^\bullet$ radicals, which possess oxidizing abilities;

$$e_{aq}^- + O_2 \rightarrow O_2^{\bullet -} \quad (4)$$

$$H^\bullet + O_2 \rightarrow HO_2^\bullet \quad (5)$$

2-propanol, as a scavenger of oxidizing radicals, hydroxyl radicals ($HO^\bullet$), was not used. However, as seen from above results gold NPs were successfully synthesized. The present PEO macromolecules in dilute solutions react with ${}^\bullet OH$ (and $H^\bullet$) radicals by hydrogen abstraction,

$$-CH_2-CH_2-O-CH_2-CH_2-O- + {}^\bullet OH\ (H^\bullet) \rightarrow -CH_2-CH_2-O-CH_2-CH^\bullet-O- + H_2O\ (H_2) \quad (6)$$

In this way PEO can to some amount act as scavenger. Obviously the PEO acting as scavenger of ${}^\bullet OH$ was enough to obtain good reducing conditions for AuNPs formation.

By increasing the Au^{3+} concentration, but with the same amount of PEO as a stabilizer, the important factor, the ratio PEO/Au decreases thus influencing size and stability of suspensions; there is not sufficient polymer to stabilize NPs. The reason for lowering of NPs size at acidic conditions can lay in the fact that at acidic conditions, the yield of e_{aq}^-, decreases, because e_{aq}^- are converted to $H^\cdot$ by reaction with H_3O^+ (Ferradini and Jay-Gerin, 2000; Spinks and Woods, 1900; Spotheim-Maurizot et al., 2008). At such reduction conditions, nuclei are formed less concentrated. Formed atoms act as nucleation centers and as „catalyst“ for the reduction of the remaining metal cations (making the redox potential

more positive) (Abidi and Remita, 2010; Gachard et al., 1988). Remaining gold cations being absorbed on clusters and reduced, thus resulting in bigger particles. In addition, the increase of NPs size at high Au^{3+} concentration can also be explained by the insufficient reduction and similar mechanism of particle formation.

Krklješ et al. (2008) observed similar effects of pH on AuNPs size obtained on γ-irradiation of PVA/Au^{3+} aqueous solutions; the biggest one synthesized at acidic conditions. In our previous work (Jurkin et al., 2016b) we reported on the influence of pH on the stability of gold nanoparticles synthesized by γ-irradiation of microemulsion; more stable AuNPs suspensions were obtained at pH < 7 than when synthesized at alkali conditions. The increase of AuNPs size, obtained on γ-irradiation of PVP/Au^{3+} solution, by increasing the Au^{III} concentration was also noted by Li et al. (2007) and Misra et al. (2012). Bigger AuNPs, as well as trigonal and hexagonal NPs were obtained by Morrow et al. (2009) for synthesis at acidic conditions (pH = 4) due to slower nucleation and hence preferential nucleation directional growth.

At alkaline conditions nanocomposite gels are formed, not suspensions. Figure 4. shows the SEM images, and the corresponding particle size distribution, of PEO/AuNPs hydrogels obtained by 50 kGy irradiation of PEO solution with 1 wt% Au^{3+} and 10 wt% Au^{3+} at pH~10.95. Particles very homogenously dispersed through polymer matrix are visible, with rare agglomerates. For gel obtained from solution with 1 wt% Au^{3+} particles of ~24 nm are embedded in PEO matrix. In gel with higher amount of AuNPs (10%) somewhat bigger (~35 nm) and slightly agglomerated particles were observed, but also particles of 100-350 nm in size, that can be NaCl particles or aggregated gold particles.

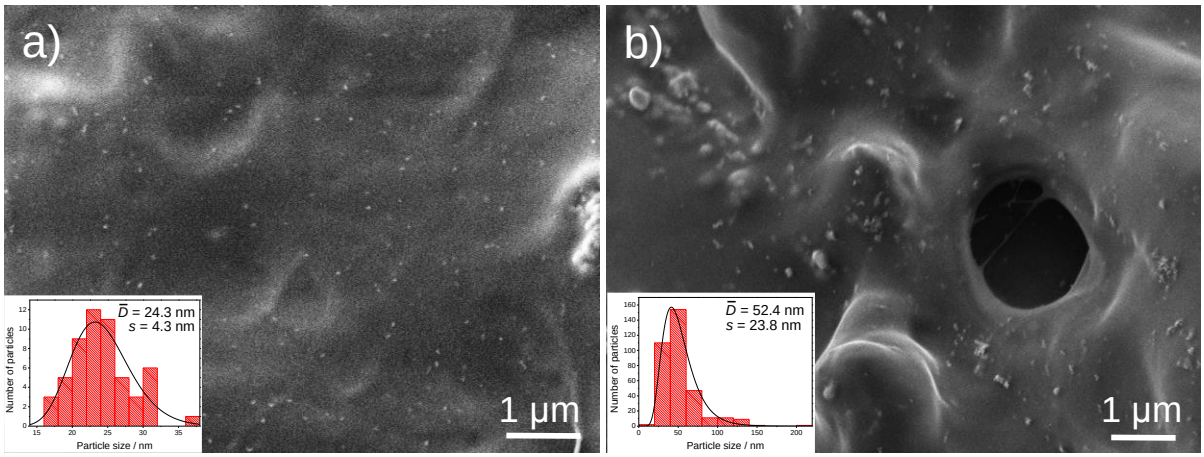

Figure 4. SEM images and corresponding particle size distributions of PEO/AuNPs hydrogels obtained by irradiation of PEO solutions with 1 wt% (a) and 10 wt% Au^{3+} (b) at pH~11. For gel obtained with 10 wt% Au^{3+} distribution of smaller particles is given; it also contained bigger aggregated/agglomerated particles.

As shown, PEO/Au nanocomposite hydrogels were successfully prepared using one-pot γ-irradiation synthesis procedure on irradiation of PEO and Au^{3+} aqueous solutions under inert atmosphere at highly alkaline conditions. The permanent shape of gels obtained is a strong evidence of a three-dimensional network and intermolecular crosslinking. At high pH crosslinking of PEO chains into macromolecular network occurred simultaneously with the reduction of Au^{3+} ions and formation of AuNPs. As mentioned before, upon irradiation of dilute PEO solution the PEO radical is not generated by direct absorption of radiation energy by PEO chains, but by reaction with hydroxyl radicals formed on water radiolysis (eq. 6) (Matheson et al., 1973; Savaş and Güven, 2002; Ulański et al., 1995a). If conditions are preferable, owing to good mobility in dilute solutions, such formed PEO macroradicals can preferably intermolecularly crosslink forming 3-D macromolecular gels.

$$2\ \text{-CH}_2\text{-}\dot{\text{C}}\text{H-O-} \longrightarrow \begin{array}{c}\text{-CH}_2\text{-CH-O-}\\ \quad\quad\quad\ |\\ \text{-CH}_2\text{-CH-O-}\end{array} \qquad (7)$$

The extent of crosslinking and the ratio of inter- and intra-molecular crosslinking depend on the irradiation conditions like dose, dose rate, atmosphere, and on concentration of PEO solution and its molecular mass (Jurkin and Pucić, 2012; Savaş and Güven, 2002; Ulański et

al., 1995a; 1995b). If additives or particles are present during the synthesis they can also influence the process of polymer crosslinking (Jurkin and Pucić, 2013).

The formation of gels at alkali conditions could be due to the increased yield of ·OH radicals at high pH (Ferradini and Jay-Gerin, 2000; Hayon, 1965; Spotheim-Maurizot et al., 2008). It has to be mentioned that there are authors observing decreasing values of ·OH yields at very high pH (Spinks and Woods, 1990; Swiatla-Wojcik, 2008). Especially for high alkaline media the question of the values of yields of some primary free radicals, like ·OH, is yet unsolved, the experimental data appearing to be contradictory. In addition, it is known that the rate constant of ·OH radicals with polymers depends on the concentration and molecular weight of polymer (PEO) (Janik et al., 1997), but also on the pH of solution. This effect of pH on the formation of gels *vs.* suspensions could also be due to the fact that by irradiation of solutions at pH < 9, depending on the $AuCl_4$ content in solution, the pH of suspension after irradiation drops below <3.5, which was shown by Charlesby and Kopp (1966) to be the critical pH, below which there was no observation of dose to gel in PEO solution. They ascribed this to a change in the shape of the PEO macromolecule, which can enhance intramolecular crosslinking at the expense of intermolecular crosslinking. The fact that PEO gels cannot be formed at pH < 3 was confirmed by additional experiment of irradiation of pure 1.85 wt% PEO aq. solution at pH = 2.97 with 50 kGy (results not shown). In addition, in acidic deoxygenated solution if chloride ions are present they can convert ·OH to $HOCl^{\cdot-}$, while in alkali ·OH can react with OH^- giving $O^{\cdot-}$ which can also abstract hydrogen form the polymer chain (Spotheim-Maurizot et al., 2008; Ferradini and Jay-Gerin, 2000).

There are several possible reasons for observed pH decrease after irradiation of $PEO/HAuCl_4$ aqueous solutions. One of the reasons is water radiolysis that results in formation of hydronium ions, H_3O^+. This would result in slight decrease of pH, not such drastic as observed in PEO/Au samples. Another reason may arise from formation of degradation products of PEO. Such significant decrease of pH (for example from pH= 8.4 to pH=4.5 depending on the irradiation time) is observed in a case of photodegradation of PEO on irradiation of its not deoxygenated aqueous solutions, and was ascribed mainly to the formation of formic acid ions, which was formed by partial hydrolysis of formates (Hassouna et al., 2007; Morlat and Gardette, 2003; Utrata-Wesołek et al., 2011). Higher rate of PEO photodegradation was observed in acidic medium (Hassouna et al., 2007) and in the presence of metal salts like $FeCl_3$ etc. (Hassouna et al., 2008). Herein, the synthesized PEO/Au samples

were obtained on γ-irradiation of deoxygenated PEO/$HAuCl_4$ aqueous solutions (bubbling with nitrogen prior to irradiation), so degradation is not expected in large amount as in oxygen, but it can still occur in some extent. Additional reason for pH decrease in PEO/Au^{3+} systems obviously lay in the presence of $HAuCl_4$ since at pH range 8-10.5 on increasing the $HAuCl_4$ concentration the formation of suspensions prevails over the formation of gels. This may be due to the chloride ions present and their reaction with the primary products of water radiolysis and/or changes of the pH during Au^{3+} reduction (like on reduction with proton radical or with some organic radicals resulting in formation of H^+). For the purpose of establishing the reasons for significant pH decrease, additional experiments were performed: *i)* the irradiation of pure MQ-water in inert atmosphere at different pH at 50 kGy slightly decreased pH, *ii)* upon irradiation of pure PEO aqueous solutions at different pH in air and nitrogen the slight decrease of pH occurred, more pronounced on irradiation in air, *iii)* upon irradiation of deoxygenated PEO/NaCl aqueous solution (with the same amount of Cl^- as in PEO/$HAuCl_4$ solution with 2wt% Au^{3+}) PEO wall-to-wall gel was formed with almost unchanged pH, and *iv)* upon irradiation of pure $HAuCl_4$ aqueous solution (without PEO) at different pH a significant decrease of pH was observed (for example from 9.38 to 3.95) (results not shown). Additional experiments confirmed above mentioned possible reasons responsible for pH decrease, as well as that the major influence is obviously due to the presence of $HAuCl_4$, however a detailed mechanism has yet to be found.

3.2 Thermal characterization of PEO/AuNPs gels

Synthetized polymer gels containing different content of AuNPs (initial 0.5, 1, 2, 5 and 10 wt% of Au^{3+} in relation to total PEO and Au mass) were characterized by differential scanning calorimetry and rheological measurements to correlate the observed rheological properties with crosslinking and hence changes in PEO crystallinity. The processes of polymer melting during heating process, as well as crystallization observed in cooling process during DSC measurements, are important because they indicate the changes of other properties like morphology or mechanical properties of polymeric materials. By investigating the thermal and rheological (mechanical) properties of nanocomposite gels the optimal concentration of nanofiller can be determined to obtain gel with the desired properties for potential application.

DSC thermographs of the second heating and the first cooling cycles of PEO/AuNPs nanocomposite gels are given in Figure 5.

Figure 6 presents the values of melting and crystallization enthalpies and temperatures of the first and the second heating and cooling cycles, as well as degree of crystallinity calculated from melting enthalpies recalculated on the pure PEO mass. The temperatures and enthalpies differ slightly for the first and second heating cycles, especially the enthalpies of melting and hence degree of crystallinity. This is due to the fact that first melting cycles are under influence of thermal and mechanical history of samples, while during the second cycles melting and crystallization occurs after controlled temperature treatment same for all the samples, so the effect of degree of crosslinking and amount of AuNPs synthesized under γ-irradiation on the melting and crystallization processes is more evident.

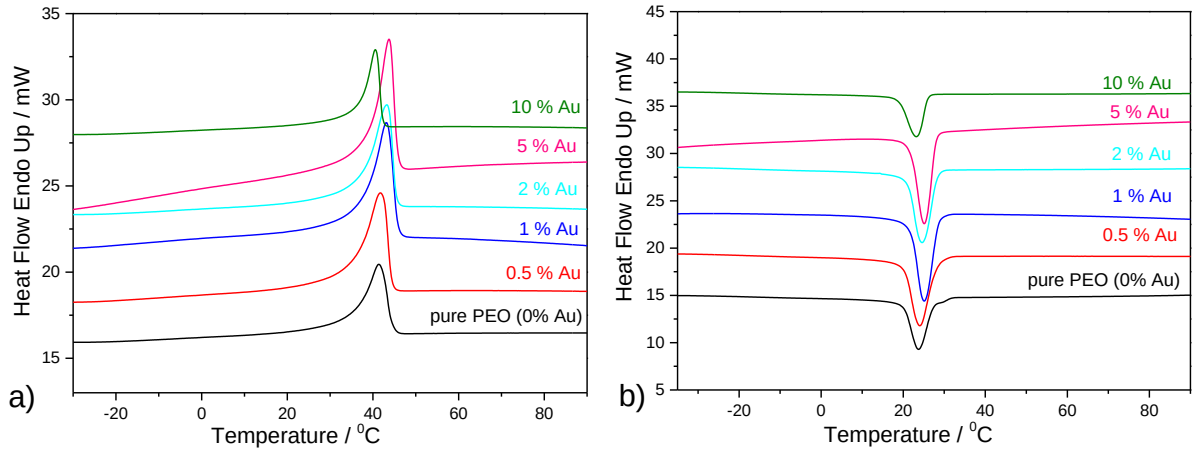

Figure 5. DSC thermographs of 2nd heating (a) and 1st cooling (b) cycles of PEO/AuNPs nanocomposite gels. Heating and cooling rates 10 °C min^{-1}.

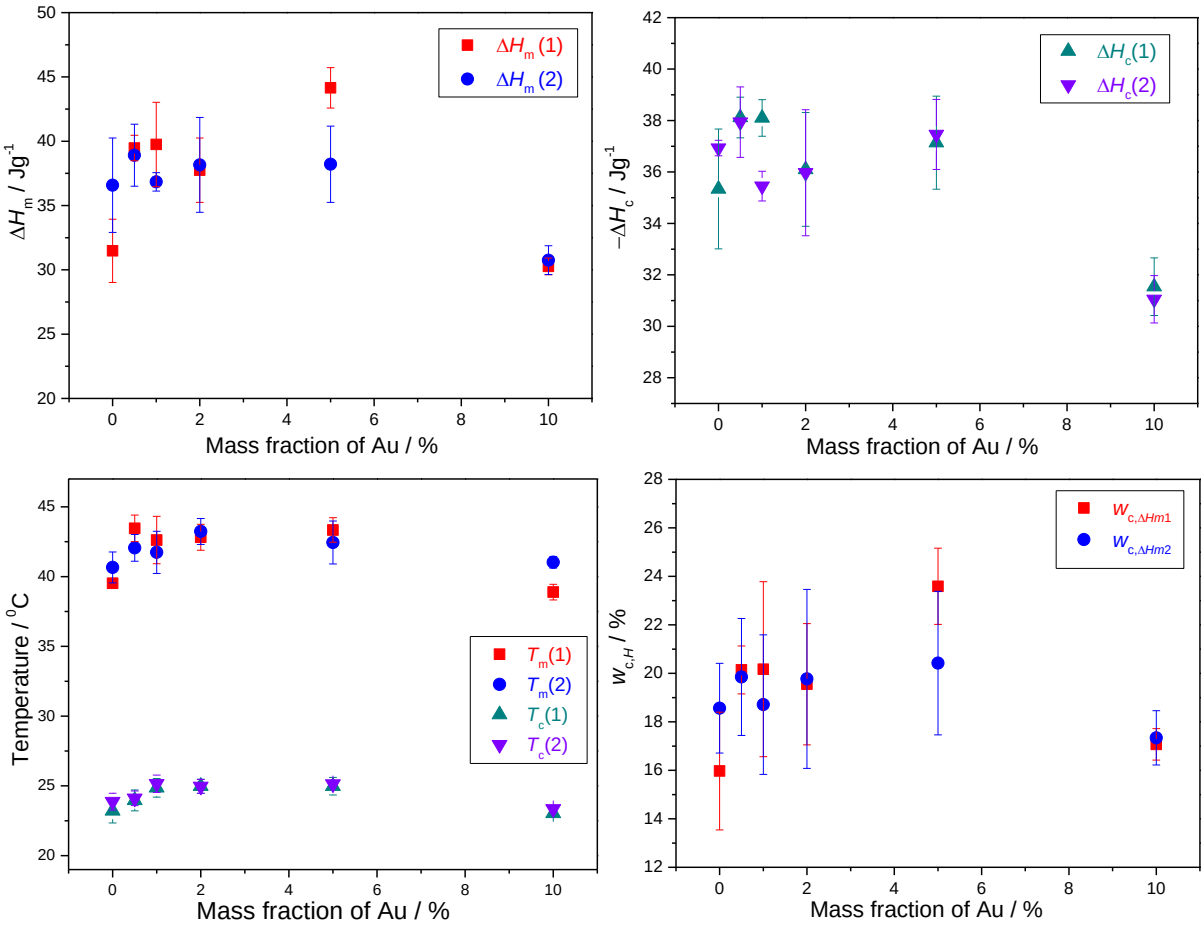

Figure 6. Melting (ΔH_m) and crystallization (ΔH_c) enthalpies and temperatures of 1st and 2nd heating and cooling cycles of PEO/AuNPs nanocomposite gels with different amount of Au (different amount of initial Au^{3+}), as well as the degree of crystallinity ($w_{c,H}$) of nanocomposite gels calculated from melting enthalpies of 1st and 2nd heating cycles recalculated on the pure PEO mass.

The enthalpies and calculated degree of crystallinity of gels revealed that at 50 kGy the density of crosslinks formed inside PEO network is still not high enough to totally prevent crystallization. Segments of PEO chains between crosslinking points inside gel can still partially crystalize on drying of gel in vacuum and during thermal treatment. The PEO/Au nanocomposite gels had generally slightly higher melting and crystallization temperatures than pure PEO gel. The AuNPs did not significantly influence phase transformation enthalpies, except for slightly lowering of enthalpies and degree of crystallinity at the highest Au loading (10 %). All gels, both pure PEO gel and nanocomposite ones, melt around 40 °C, and crystalize around room temperatures.

Both the temperatures and the enthalpies of melting and crystallization showed the stepwise behavior on increase of AuNPs content. Firstly, an increase of enthalpies and temperatures occurred at small amount of AuNPs (increased enthalpies up to 1 wt% Au for first cycles and 0.5% Au for second cycles). At 2% AuNPs the values decreased, followed by the second increase of enthalpies and temperatures at 5 % Au. The lowest values were observed for 10 % AuNPs loading.

DSC measurements revealed that simultaneous synthesis of PEO/Au nanocomposite gels resulted in nanocomposite gels with no significantly changed thermal properties compared to pure PEO gel. That is, simultaneous synthesis of AuNPs on irradiation did not drastically influence concurrent crosslinking process of PEO chains. Besides, afterwards on drying in vacuum and during the thermal treatment in DSC formed AuNPs did not considerably affect crystallization and melting process of nanocomposite gels. Though, some effect of amount of AuNPs is observable. The nucleation effect of filler at lower amount of AuNPs, what resulted in increased temperatures of crystallization, is most pronounced up to 1%. Fillers increase the density of nucleation centers and promote the heterogeneous nucleation in polymer gels. This results in easier crystallization of partially crosslinked PEO chains and in formation of smaller and less „perfect“ spherulites. Hence, the T_c increases. At 0.5% of AuNPs nucleation effect obviously resulted in smaller but better structurated crystallites and hence higher enthalpies then pure PEO gel. At 1% there is a very strong nucleation effect of filler, as shown by highest T_c and decrease in enthalpies and T_m. This is because, generally, smaller spherulites and crystallites are less "perfect" (less structurated) than bigger ones, so they melt at lower temperatures. Obviously, at lower AuNPs concentrations because of the small amount of formed AuNPs and their homogenous distribution through polymer matrix (as observed on SEM image Figure 4a) crystallization process of PEO chains is not hindered, it is even triggered. The lowest values of enthalpies, crystallinity degree and temperatures were observed for the gel containing highest Au loading of 10 %, even slightly lower that for pure PEO gel. This could be due to the interactions between NPs present in high amount and partially crosslinked PEO chains, thus reducing mobility of PEO chains. Also, the highest amount of NPs, due to somewhat worsened dispersion and partial NPs agglomeration, can restrain mobility of partially crosslinked PEO chains and its crystalizability, resulting in lowering of crystallization temperatures and degree of crystallinity. Filler agglomerates can also be an obstacle for PEO crosslinking, as noted in our older work in the case of silica NPs (Jurkin and Pucić, 2013). Although some

agglomeration at highest AuNPs content is expected and is confirmed by SEM microscopy (Figure 4b) it did not have significant influence on enthalpies and phase transformations temperatures compared to pure PEO gel.

Krklješ et al. (2007) observed the similar behavior of PVA/Ag gels which showed T_m decreased with the increase of Ag content compared to pure PVA gel, with a very small T_m increase up to 1 wt% of Ag, and the highest degree of crystallinity for 1 wt% of Ag, with the further increase of Ag concentration degree of crystallinity lowered.

3.3 Rheological properties of PEO/AuNPs gels

The viscoelastic properties of gels are described using oscillatory rheology. During the amplitude test, the frequency is held constant and the shear strain is varied. Storage modulus *G*' represents the stored deformation energy and loss modulus *G*" characterizes the deformation energy dissipated through internal friction when flowing. For gels, the elastic component dominates (G') over viscous component (G'') at small applied shear and attains a plateau in the linear response region (LVR or linear viscoelastic region). The amplitude sweep tests of pure PEO gel and nanocomposite gels are shown in Figure 7 and results given in Table 2. All investigated gels behave like viscoelastic solids with G' values much higher than G'' values indicating solid-like behavior and confirming well-ordered gel network. The values of storage modulus had the maximum at concentration of 1 wt % Au in PEO matrix, while the values of yield point and flow point had maximum at 0.5 wt% Au. After that, constant decrease of viscoelastic properties till concentration of 10 wt% of AuNPs was observed.

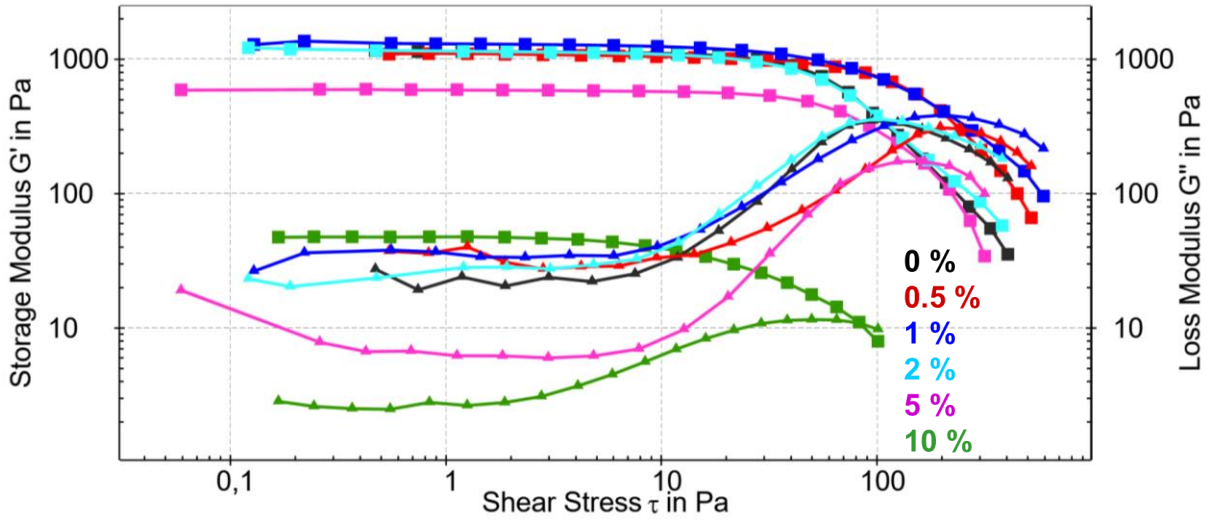

Figure 7. Amplitude sweep test (G' (■) and G'' (▲) values) of pure PEO gel and nanocomposite gels containing 0.5 wt%, 1 wt%, 2 wt%, 5 wt% and 10 wt% of Au (initial wt% Au^{3+} in relation to total PEO and Au mass) at constant frequency of 5 rad/s at 25 °C.

Table 2. Results of amplitude sweep test of pure PEO gels and PEO/Au nanocomposite gels.

Percentage by mass of Au* / %	G' (max) / Pa	Yield point / Pa	Flow point / Pa	Flow transition index
0	1157	42.2	105.8	2.5
0.5	1091	**74.8**	**239.5**	3.2
1	**1313**	43.7	218.5	5.0
2	1187	33.8	103.4	3.1
5	597	39.6	162	4.1
10	47.7	9.2	83.6	9.1

*wt% of Au^{3+} in relation to total PEO and Au mass

G' values of gels were in decreasing order: 1% > 0% ≈ 2% > 0.5% >> 5% > 10% Au. For NPs loading up to 2 % G' were above 1 kPa. The strength of nanocomposite gels with loading of AuNPs up to 1 % compared to pure PEO gel was improved. The yield point value (74.8 Pa) of gel with 0.5 % Au was almost two times higher, and the flow point value more than two times higher (239 Pa) compared to pure PEO gel. At other Au content flow points showed this decreasing order: 0.5% > 1% > 5% > 0% ≈ 2% >> 10 % Au. Also, yielding zone, a valley between yield point and flow point values, shows influence of AuNPs on gel network formation. For pure PEO gel a flow transition index had the smallest value of 2.5, compared

with much higher values for nanocomposite gels, especially one with 10 % Au (wide yielding zone, 9.1), indicating different microstructure of network. Nanocomposite gels showed continuous decrease of microstructure strength compared to faster change of pure PEO gel structure. All the results indicate strong influence of amount of AuNPs, and consequently of NPs distribution inside the gel, on the viscoelastic properties. Specifically, at initial 0.5 % Au^{3+} nanocomposite gel was formed with similar *G*' value compared to pure PEO gel, but with exceptionally strong influence on microstructure elasticity of gel with two times higher yield and flow point values. This confirms well-ordered gel network formation of PEO and indicates good filler (NPs) dispersion at this low amount of AuNPs. Small amounts of AuNPs up to 1% were beneficial for increasing the elasticity of gel, increasing the overall strength of the gel and yield and flow points, since, in addition to reinforcing effect of filler, the crosslinking of PEO chains is not yet hindered by NPs and strong polymer network is still formed. At 2 % filler the gel starts to soften by all parameters. Still, strong gel was formed at 2 % Au, but with significantly lower values of yielding zone and flow point compared to 0.5% and 1% gels. The properties of the gel with 2% AuNPs is more likely to compare with pure PEO gel. Almost the same quantities of *G*' values and flow point values were noticed for 2% loading of AuNPs and pure PEO gel. The gel strength is still preserved but the indicative parameter that internal structure is disrupted at the micro-level is seen through the significantly lower value of yield point for the 2% loading of AuNPs. At this point it is reasonable to conclude that initial agglomeration of AuNPs starting to influence the crosslinking of PEO chains, but the microstructure of gel is still rather stable. On contrary, at 5 % Au, due to relatively high loading of NPs, yield point and flow point increases but the overall influence on gel strength was lower (*G*' value). A gel strength at 10% of Au loading was exceptionally low, also the low values of all other viscoelastic parameters indicate not properly formed polymer network probably due to presence of high amount of NPs and agglomerates, as also noticed on SEM image (Figure 4b).

The quantity loss factor, $\tan(\delta) = G''/G'$, determines the relative elasticity of viscoelastic materials. The gels with a value of $\tan(\delta) = 0.1$ and lower belong to stiff gels. All investigated nanocomposite gels showed low loss factor values, determined in LVR, in range from 0.01 up to 0.05, which is indicative of a high relative elastic modulus and well-ordered gel systems. Loss factor for pure PEO gel and gels with loaded Au concentration from 0.5 % up to 2 % was similar ~ 0.02. Samples loaded with 5 % Au showed somewhat lower values of

loss factor (0.01), hence more ordered structure, while the sample doped with 10% Au had the highest value (0.05).

Overall, the observed improvement in properties of gels (stronger gels with higher flow points and G' values), with 0.5% and 1% Au, and more ordered structure as indicated by higher values of loss factor and flow point at 5% of the filler, can also be observed on DSC thermograms as an increase in crystallization temperatures due to the good nucleation effect of filler at this concentrations, as well as in maxima of enthalpies and degree of crystallinity. This can be explained by very good dispersion of filler at these concentrations, resulting in better structuring of partially crosslinked PEO chains, better ordering of the system, and good transfer of stress from polymer chains to the filler (due to interactions of NPs and polymer and homogeneous NPs dispersion). The worst rheological properties of gel with 10 % Au (lowest storage modulus, yield point and flow point), which are in line with the lowest values of phase transformation temperatures, enthalpies and degree of crystallinity, are probably due to the worsened dispersion of AuNPs through the gel and NPs agglomeration sterically preventing the polymer chains to crosslink.

Jovanović et al. (2011) and Spasojević et al. (2015) also observed formation of stronger gels, and in a case of PVP less elastic gels, on incorporation of smaller amount of Ag NPs by *in situ* radiolytical reduction in PVP and PNIPAM gels, respectively.

Frequency sweeps describe the time-dependent behavior of a sample in the non-destructive deformation range, gathering information on the behavior and inner structure of polymer/network, and system homogeneity. Frequency sweep studies (ω = 0.05−100 rad/s at 0.8% strain, LVR) of investigated gels at 25 °C confirmed the "solid-like" behavior for all gels and showed that the storage modulus (G') and loss modulus (G'') values are mostly independent of the applied frequency within the linear viscoelastic regions (LVRs) (Figure 8). The investigated samples are true chemically crosslinked gels. G' values (the elastic component of the gel) were constant through entire frequency range for all gels. The G' value at lower frequency can be used for comparison of the crosslinking density of different samples. The higher the G' value, the higher the degree of crosslinking (Mezger, 2014). This also confirmed the high crosslinking degree for 0.5% AuNPs loading, while at 10% AuNPs loading, due to high particle concentration and partial agglomeration, crosslinking degree is lower. A pure PEO gel and all nanocomposite gels, except of 10 wt% Au gel, showed small changes in loss factor at frequencies below 0.2 rad/s, due to change of loss modulus G''. The

time dependent behavior of nanocomposite gels were similar to pure PEO gel, except for 10 wt% loaded gel were the same stability was obtained throughout examined frequency range. The gel with 10 % of AuNPs loading was very soft, but despite to 20 times lower *G'* value compared with pure PEO and PEO gels loaded with up to 1% of AuNPs, the exceptional stability at lower frequencies showed good homogeneity of the system, good distribution of Au nanoparticles and agglomerates within PEO matrix through prolonged period of time. It is known that the high concentrated and highly agglomerated systems show minimal variation of storage modulus with frequency (Shenoy, 1999).

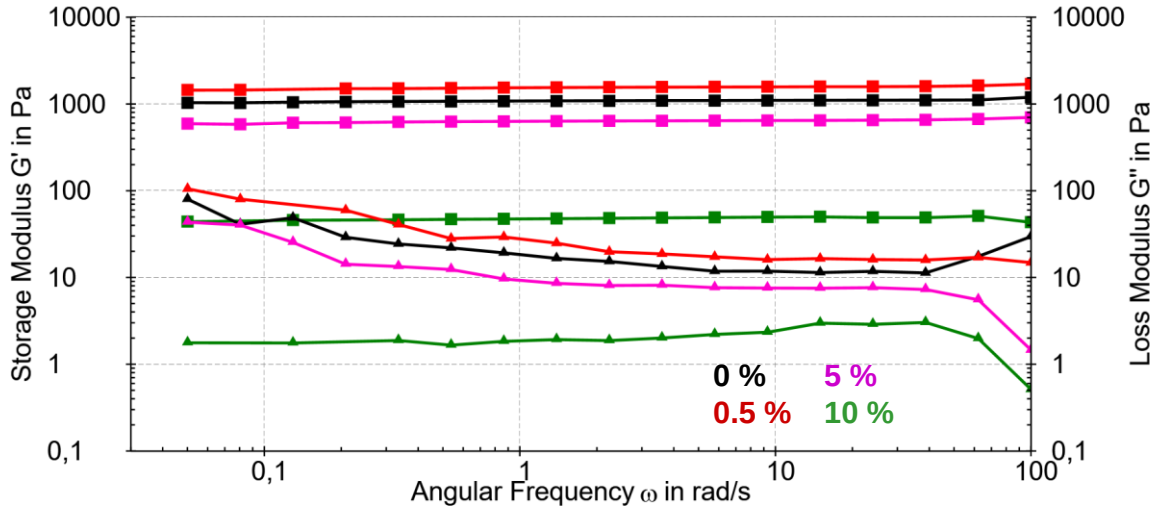

Figure 8. Frequency sweep tests (G′ (■) and G″ (▲) values) (frequency range 0.05-100 rad/s, strain at LVR) of pure PEO gel and nanocomposite gels containing 0.5 wt%, 5 wt% and 10 wt% of Au (initial wt% Au^{3+}) at 25 °C.

Thixotropy is a time-dependent phenomenon, as the viscosity of the substance has to recover after a certain period of time when the applied stress is removed. In thixotropic materials the structural strength decreases (structural breakdown) while shearing and recovers after a certain rest period (structural recovery). In the thixotropic experiments, rheological measurements were conducted under initial conditions at which they were in their linear viscoelastic regimes (a strain of 0.5 % and angular frequency of 5 rad/s) for 680 s to establish baseline values for *G′* and *G″*. After that, destructive strain of 300 % for 60 s at angular frequency 5 rad/s and additional 680 s of non-destructive strain (0.5 % at 5 rad/s) were

applied. Viscoelastic recovery of gels was observed after the cessation of destructive strain (Figure 9). Figure 9a shows the evolution of G' and G'' for pure PEO and PEO/Au nanocomposite gels after applying a destructive strain, a condition that leads to loss of its viscoelasticity. The sample behavior switched from gel-like to sol-like, with G'' values higher that G'. After that, the original conditions were reapplied in order to monitor the recovery of the viscoelastic properties of the gels. All investigated gels revealed excellent recovery properties (self-healing properties) (Figure 9). In less than 10 seconds all gels exhibited a recovery ratio of 90 %. After 60 seconds pure PEO gel recovers to 92 %, one with 0.5 % Au to 96 %, 1% Au to 91%, 2% Au to 92 %, 5% Au to 91% and 10% of Au to 94 % recovery. Again, best recovery ratio was observed for gel with 0.5 wt% Au. Excellent recovery properties of all gels indicates very good microstructure integrity. This also confirms that the incorporation of nanoparticles did not significantly altered the gel structure, even at the highest AuNPs amount. Moreover, the NPs concentration of 0.5% resulted in a stronger gel, with good elasticity, higher flow point and yield point and somewhat better recovery than pure PEO gel. Excellent recovery ratio could is also indication of good NPs dispersion within the polymer gel as well as it could be indication of good interactions between NPs and polymer.

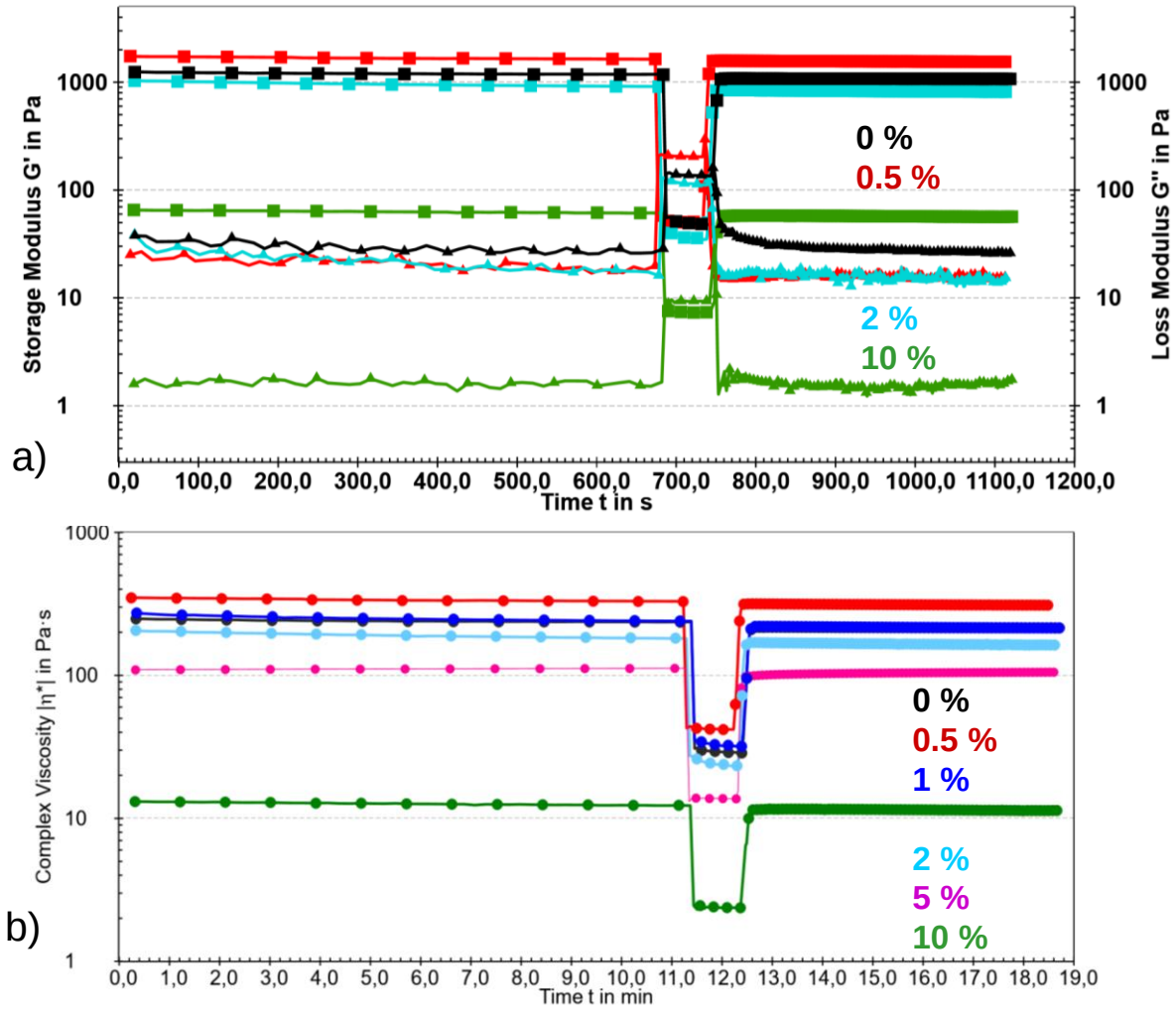

Figure 9. 3ITT thixotropy test of pure PEO gel and nanocomposite gels containing 0.5 wt%, 1 wt%, 2 wt%, 5 wt% and 10 wt% of Au (initial wt% Au^{3+} in relation to total PEO and mass) presented as: a) storage G' (■) and loss G'' (▲) modulus and b) complex viscosity (η^*) as a function of time and application of different strains at 25 °C.

Both DSC and rheological measurements indicate that an optimal amount (at 50 kGy) for incorporating AuNPs and still preserving good viscoelastic properties, or even obtaining better properties (stronger gels, better viscoelastic properties, higher storage modulus, better recovery) of such composite gel comparing to pure PEO gel is up to 1 wt%. Higher filler loading exhibited worsening of properties (lowest storage modulus, yield point and flow point) probably due to possible worsened dispersion and agglomeration of AuNPs, being an obstacle for crosslinking of PEO chains. Still, all nanocomposite gels, even one with highest amount of AuNPs, showed excellent recovery properties and stability.

The obtained PEO/AuNPs nanocomposite gels showed promising rheological properties for potential application in tissue engineering and as wound dressings, but further optimization of irradiation conditions as well as precursor solution conditions is necessary.

4. Conclusions

By optimizing the pH, PEO/Au^{3+} ratio and Au^{3+} concentration of precursor solution stable Au suspension or PEO/AuNPs hydrogels can be obtained on irradiation. The pH was a crucial factor in determining formation of suspension *vs.* gels.

The final size of gold nanoparticles and stability of suspensions markedly depended on pH of solution, but also on precursor Au^{3+} concentration. Neutral pH favored formation of stable Au suspensions with small NPs. Bigger AuNPs and unstable suspensions were formed at more acidic conditions and by increasing initial Au^{3+} concentration.

γ-irradiation method showed to be an effective and suitable method for one-step synthesis of PEO/AuNPs nanocomposite hydrogels, at alkaline conditions. On γ-irradiation crosslinking of PEO with the formation of network occurred simultaneously with formation of Au nanoparticles. AuNPs of small size were obtained, well dispersed through polymer matrix.

Thermal and viscoelastic properties of the gels depended on the amount of AuNPs synthesized inside gels.

The optimal amount was up to 1 wt% Au^{3+} for incorporating AuNPs and preserving or even obtaining better properties (stronger gels, higher storage modulus, higher yield point and flow point, better recovery) than pure PEO gels. Higher amount of NPs did not result in enhancing strength of gel, probably because of agglomeration of AuNPs being an obstacle for crosslinking of PEO chains. All nanocomposite gels showed excellent recovery properties and stability.

Obtained nanocomposite gels showed promising rheological properties for potential application, but further optimization is necessary.

Acknowledgments

This work was financially supported by the Croatian Science Foundation under the project UIP-2017-05-7337 “The impact of polymers on the radiolytic synthesis of magnetic nanoparticles” (POLRADNANOP).

References

Abidi, W., Remita H., 2010. Gold based nanoparticles generated by radiolytic and photolytic methods. Rec. Patent. Eng. 4, 170–188.

Al Gharib, S., Marignier, J.-L., El Omar, A.K., Naja, A., Le Caer, S., Mostafavi, M., Belloni, J., 2019. Key role of the oxidized citrate-free radical in the nucleation mechanism of the metal nanoparticle Turkevich synthesis, J. Phys. Chem. C, 123, 22624–22633.

Belloni, J., Mostafavi, M., Remita, H., Marignier, J.-L., Delcourt, M.-O., 1998. Radiation-induced synthesis of mono- and multi-metallic clusters and nanocolloids. New. J. Chem. 22, 1239–1255.

Butterworth, K.T., McMahon, S.J., Currell, F.J., Prise, K.M., 2012. Physical basis and biological mechanism of gold nanoparticle radiosensitization. Nanoscale 4, 4830–4838.

Charlesby A., Kopp, P.M., 1966. Radiation protection of aqueous polyethylene oxide solutions by thiourea. Proc. Roy. Soc. (London), Ser. A. 291, 129–143.

Dey, G.R., El Omar, A.K., Jacob, J.A., Mostafavi, M., Belloni, J., 2011. Mechanism of trivalent gold reduction and reactivity of transient divalent and monovalent gold ions studied by gamma and pulse radiolysis. J. Phys. Chem. A, 115, 383–391.

Dykman L., Khlebtsov, N., 2012. Gold nanoparticles in biomedical applications: recent advances and perspectives. Chem. Soc. Rev. 41, 2256–2281.

Ferradini C., Jay-Gerin, J.-P., 2000. The effect of pH on water radiolysis: a still open question – a minireview. Res. Chem. Intermed. 26 (6) 549–565.

Gachard, E., Remita, H., Khatouri, J., Keita, B., Nadjo, L., Belloni, E., 1998. Radiation-induced and chemical formation of gold clusters. New. J. Chem. 1257–1265.

Gotić, M., Jurkin, T., Musić, S., 2009. From iron(III) precursor to magnetite and *vice versa*. Mater. Res. Bull. 44, 2014–2021.

Hainfeld, J.F., Slatkin D.N., Smilowitz, H.M., 2004. The use of gold nanoparticles to enhance radiotherapy in mice. Phys. Med. Biol. 49, N309–N315.

Hainfeld, J.F., Slatkin D.N., Focella T.M., Smilowitz, H.M., 2006. Gold nanoparticles: a new X-ray contrast agent. Br. J. Radiol. 79, 248–253.

Haiss, W., Thanh, N.T.K., Aveyard, J., Feming, D.G., 2007. Determination of size and concentration of gold nanoparticles from UV-vis 0spectra. Anal. Chem. 79, 4215–4221.

Hanžić, N., Horvat, A., Bibić, J., Unfried, K., Jurkin, T., Dražić, G., Marijanović, I., Slade, N., Gotić, M., 2018. Syntheses of gold nanoparticles and their impact on the cell cycle in breast cancer cells subjected to megavoltage X-ray irradiation. Mater. Sci. Eng. C 91, 486–495.

Hanžić, N., Jurkin, T., Maksimović, A., Gotić, M., 2015. The synthesis of gold nanoparticles by a citrate radiolytical method. Radiat. Phys. Chem. 106, 77–82.

Hasan, A., Morshed, M., Memic, A., Hassan, S., Webster, T.J., Marei H.E.-S., 2018. Nanoparticles in tissue engineering: applications, challenges and prospects. Int. J. Nanomed. 13, 5637–5655.

Hassouna, F., Mailhot, G., Morlat-Thérias, S., Gardette, J.-L., 2008. Photochemical behaviour of poly(ethylene oxide) (PEO) in aqueous solution: Influence of iron salts. J. Photoch. Photobio. A 195, 167–174.

Hassouna, F., Morlat-Thérias, S., Mailhot, G., Gardette, J.L., 2007. Influence of water on the photodegradation of poly(ethylene oxide). Polym. Degrad. Stabil. 92, 2042–2050.

Hayon, E., 1965. Radical and molecular yields in the radiolysis of alkaline aqueous solutions. Trans. Faraday Soc. 61, 734–743.

Hoppe, C.E., Lazzari, M., Pardiñas-Blanco, I., Lopez-Quintela, M.A., 2006. One-step synthesis of gold and silver hydrosols using poly(N-vinyl-2-pyrrolidone) as a reducing agent. Langmuir 22, 7027–7034.

Ide, M.S., Davis, R.J., 2014. The important role of hydroxyl on oxidation catalysis by gold nanoparticles. Acc. Chem. Res. 47, 825–833.

Jahangirian, H., Kalantari, K., Izadiyan, Z., Rafiee-Moghaddam, R., Shameli, K., Webster, T.J., 2019. A review of small molecules and drug delivery applications using gold and iron nanoparticles. Int. J. Nanomed. 14, 1633–1657.

Jain, S., Coulter J.A., Hounsell, A.R. et al., 2011. Cell-specific radiosensitization by gold nanoparticles at megavoltage radiation energies. Int. J. Radiat. Oncol. Biol. Phys. 79, 531–539.

Janik, I., Kujawa, P., Ulanski, P., Rosiak J.M., 1997. Pulse radiolysis of polymers in aqueous solution. Kinetics study. J. Chim. Phys. 94, 244–250.

Jiao, P.F., Zhou, H.Y., Chen, L.X., Yan, B., 2011. Cancer-targeting multifunctionalized gold nanoparticles in imaging and therapy. Curr. Med. Chem. 18, 2086–2102.

Jovanović, Ž., Krklješ, A., Stojkovska, J., Tomić, S., Obradović, B., Mišković-Stanković, V., Kačarević-Popović, Z., 2011. Synthesis and characterization of silver/poly(*N*-vinyl-2-pyrrolidone) hydrogel nanocomposite obtained by *in situ* radiolytic method. Radiat. Phys. Chem. 80, 1208–1215.

Jurkin, T., Guliš, M., Dražić, G., Gotić, M., 2016b. Synthesis of gold nanoparticles under highly oxidizing conditions. Gold Bull. 49, 21–33.

Jurkin, T., Pucić, I., 2013. Irradiation effects in poly(ethylene oxide)/silica nanocomposite films and gels. Polym. Eng. Sci. 53 (11) 2318–2327.

Jurkin, T., Pucić, I., 2012. Poly(ethylene oxide) irradiated in the solid state, melt and aqueous solution – a DSC and WAXD study. Radiat. Phys. Chem. 81, 1303–1308.

Jurkin, T., Štefanić, G., Dražić, G., Gotić, M., 2016a. Synthesis route to δ-FeOOH nanodiscs. Mater. Lett., 173, 55–59.

Khlebtsov, N.G., 2008. Determination of size and concentration of gold nanoparticles from extinction spectra. Anal. Chem. 80, 6620–6625.

Krklješ, A., Kačarević-Popović, Z.M., 2007. Thermal properties of radiolytically synthesized PVA/Ag nanocomposites. Hem. Ind. 61, 129–134.

Krklješ, A., Mitrić, M., Kačarević-Popović, Z., 2008. Radiolytic synthesis and characterization of PVA/Au nanocomposites: The influence of pH values. Hem. Ind. 62, 101–106.

Kwon, M.J., Lee, J., Wark, A.W., Lee, H.J., 2012. Nanoparticle-enhanced surface plasmon resonance detection of proteins at attomolar concentrations: comparing different nanoparticle shapes and size. Anal. Chem. 84; 1702–1707.

Li, T., Park, H.G., Choi, S.-H., 2007. γ-Irradiation-induced preparation of Ag and Au nanoparticles and their characterizations. Mater. Chem. Phys. 105, 325–330.

Llevot, A., Astruc, D., 2012. Application of vectorised gold nanoparticles to the diagnostic and therapy of cancer. Chem. Soc. Rev. 41, 242–257.

Marić, I., Štefanić, G., Gotić, M., Jurkin, T., 2019. The impact of dextran sulfate on the radiolytic synthesis of magnetic iron oxide nanoparticles, J. Mol. Struct. 1183 (2019) 126–136.

Matheson, M.S., Mamou, A, Silverman, J., Rabani, J., 1973. Reaction of hydroxyl radicals with polyethylene oxide in aqueous solution. J. Phys. Chem. 77 (20) 2420–2424.

Menczel J.D., Prime R.B., 2009. Thermal Analysis of Polymers. Fundamentals and Applications, John Wiley & Sons, Inc., Hoboken, New Jersey, pp. 111.

Mezger, T .G., 2014. Applied Rheology, Anton Paar GmbH, Graz, pp. 117.

Mikac, L., Marić, I., Štefanić, G., Jurkin, T., Ivanda, M., Gotić, M. 2019. Radiolytic synthesis of manganese oxides and their ability to decolorize methylene blue in aqueous solutions, Appl. Surf. Sci. 476, 1086–1095.

Misra, N., Biswal, J., Gupta, A., Sainis, J.K., Sabharwal, S., 2012. Gamma radiation induced synthesis of gold nanoparticles in aqueous polyvinyl pyrrolidone solution and its application for hydrogen peroxide estimation. Radiat. Phys. Chem. 81, 195–200.

Morlat, S., Gardette, J-L., 2003. Phototransformation of water-soluble polymers. Part II. photooxidation of poly(ethylene oxide) in aqueous solution. Polymer 44, 7891–7897.

Morrow, B.J., Matijević, E., Goia, D.V., 2009. Preparation and stabilization of monodisperse colloidal gold reduction with amonodextran. J. Colloid. Interface. Sci. 62–69.

Navaei, A., Saini, H., Christenson, W., Sullivan, R.T., Ros, R., Nikkhah, M., 2016. Gold nanorod-incorporated gelatin-based conductive hydrogels for engineering cardiac tissue constructs. Acta Biomater. 41, 133–146.

Nirwan, V.P., Al-Kattan, A., Fahmi, A., Kabashin, A.V., 2019. Fabrication of stable nanofiber matrices for tissue engineering via electrospinning of bare laser-synthesized Au nanoparticles in solution of high molecular weight chitosan. Nanomaterials 9, 1058.

Savaş H., Güven, O., 2002. Gelation, swelling and water vapor permeability behavior of radiation synthesized poly(ethylene oxide) hydrogels. Radiat. Phys. Chem. 64, 35–40.

Ravichandran, R., Sridhar, R., Venugopal, J.R., Sundarrajan, S., Mukherjee, S., Ramakrishna, S., 2014. Gold nanoparticle loaded hybrid nanofibres for cardiogenic differentiation of stem cells for infarcted myocardium regeneration. Macromol. Biosci. 14, 515–525.

Reuveni, T., Motiei, M., Romman, Z., Popovtzer, A., Popovtzer, R., 2011. Targeted gold nanoparticles enable molecular CT imaging of cancer: an in vivo study. Int. J. Nanomed. 6, 2859–2864.

Rojanathanes R., Sereemaspun, A., Pimpha, N., Buasorn, V., Ekawong P., Wiwanitkit, V., 2008. Gold nanoparticles as an alternative tool for a urine pregnancy test. Taiwan J. Obstet. Gynecol. 47, 269–299.

Rosa, S., Connolly C., Schettino G., Butterworth, K.T., Prise K.M., 2017. Biological mechanisms of gold nanoparticle radiosensitization, Cancer Nanotech. 8, 2.

Shenoy, A.V., 1999. Rheology of filled systems, Springer-Science+Business Media, B.V, Dordrecht, originally published by Kluwer Academic Publishers, pp. 222, 349, 358–360.

Shevach M., Fleischer, S., Shapira, A. Dvir, T., 2014. Gold nanoparticle-decellularized matrix hybrids for cardiac tissue engineering. Nano Lett. 14, 5792–5796.

Spasojević, J., Radosavljević, A., Krstić, J., Jovanović, D., Spasojević, V., Kalagasidis-Krušić, M., Kačarević-Popović, Z., 2015. Dual responsive antibacterial Ag-poly(N-isopropylacrylamide/itaconic acid) hydrogel nanocomposites synthesized by gamma irradiation. Europ. Polym. J. 69, 168–185.

Spinks J.W.T., Woods, R.J. 1990. Introduction to radiation chemistry. Third edition. John Wiley & Sons, New York, pp. 262.

Spotheim-Maurizot, M., Mostafavi, M., Douki T., Belloni, J., 2008. Radiation chemistry. From basics to application in material and life sciences. EDP Sciences, Les Ulis Cedex A, France, pp. 8,9, 83 and 121.

Swiatla-Wojcik, D. 2008. Computation of the effect of pH on spur chemistry in water radiolysis at elevated temperatures. Nukleonika, 53, S31–S37.

Thoniyot, P., Tan, M.J., Karim, A.A., Young, D.J., Loh, X.J., 2015. Nanoparticle-Hydrogel composites: concept, design, and applications of these promising, multifunctional materials. Adv. Sci. 2, 1400010.

Tiwari, P.M., Vig, K., Dennis, V.A., Singh, S.R., 2011. Functionalized gold nanoparticles and their biomedical applications. Nanomaterials 1, 31–63.

Ulański P., Zainuddin, Rosiak, J.M., 1995a. Pulse radiolysis of poly(ethylene oxide) in aqueous solutions. I. Formation of macroradicals. Radiat. Phys. Chem. 46, 913–916.

Ulański P., Zainuddin, Rosiak, J.M., 1995b. Pulse radiolysis of poly(ethylene oxide) in aqueous solutions. II. Decay of macroradicals. Radiat. Phys. Chem. 46, 917–920.

Utrata-Wesołek, A., Trzcińska, R., Galbas, K., Trzebicka, B., Dworak, A., 2011. Photodegradation of polyglycidol in aqueous solutions exposed to UV irradiation. Polym. Degrad. Stabil. 96, 907–918.

Wunderlich, B., 1973. Macromolecular Physics, Academic Press, New York, pp. 398 (vol. 1) and pp. 67 (vol.3)

Zhu, J., Ye, Z., Fan, X., Wang, H., Wang, Z., Chen, B., 2019. A highly sensitive biosensor based on Au NPs/rGO-PAMAM-Fc nanomaterials for detection of cholesterol. Int. J. Nanomed. 14, 835–849.

Zope, B.N., Hibbitts, D.D., Neurock, M., Davis, R.J., 2010. Reactivity of the gold/water interface during selective oxidation catalysis. Science 330, 74–78.